

Radionuclides in primary coolant of a fluoride salt-cooled high-temperature reactor during normal operation

Guo-Qing Zhang¹ · Shuai Wang¹ · Hai-Qing Zhang¹ · Xing-Wang Zhu¹ · Chao Peng^{1,2} · Jun Cai¹ · Zhao-Zhong He¹ · Kun Chen¹

Received: 3 September 2015 / Revised: 25 November 2015 / Accepted: 9 December 2015 / Published online: 17 February 2017
© Shanghai Institute of Applied Physics, Chinese Academy of Sciences, Chinese Nuclear Society, Science Press China and Springer Science+Business Media Singapore 2017

Abstract The release of fission products from coated particle fuel to primary coolant, as well as the activation of coolant and impurities, were analysed for a fluoride salt-cooled high-temperature reactor (FHR) system, and the activity of radionuclides accumulated in the coolant during normal operation was calculated. The release rate (release fraction per unit time) of fission products was calculated with STACY code, which is modelled mainly based on the Fick's law, while the activation of coolant and impurities was calculated with SCALE code. The accumulation of radionuclides in the coolant has been calculated with a simplified model, which is generally a time integration considering the generation and decay of radionuclides. The results show that activation products are the dominant gamma source in the primary coolant system during normal operation of the FHR while fission products become the dominant source after shutdown. In operation condition, health-impacts related nuclides such as ³H, and ¹⁴C originate from the activation of lithium and coolant impurities including carbon, nitrogen, and oxygen. According to the calculated effective cross sections of neutron activation, ⁶Li and ¹⁴N are the dominant ³H production source and ¹⁴C

production source, respectively. Considering the high production rate, ³H and ¹⁴C should be treated before being released to the environment.

Keywords Source term · FHR · Primary coolant · Fick's law · Diffusion

1 Introduction

The concept of FHR was first proposed at the Oak Ridge National Laboratory (ORNL) in 2003 [1]. FHR makes use of triple-isotopic (TRISO)-coated particle fuel [2] developed originally for high-temperature reactors, and fluoride salt coolant (chemical composition: 2LiF–BeF₂). At the Shanghai Institute of Applied Physics (SINAP), Chinese Academy of Sciences, a test pebble-bed FHR is now under development [3]. The test reactor has a designed thermal power of 10 MW, and it is molten-salt cooled and graphite moderated. General design parameters of the test FHR are listed in Table 1.

The pebble fuel used in the test FHR makes use of the TRISO particle (Fig. 1) which consists of a UO₂ fuel kernel within multiple coating layers to prevent the leakage of radioactive materials at temperatures up to 1600 °C [4]. In fuel pebbles, TRISO particles distribute in the graphite matrix inside a 0.5 cm thick graphite shell. The pebble has a diameter of 6 cm and a uranium loading of 7 g with the ²³⁵U enrichment of 17.08%. In the fuel region, pebbles are uniformly (randomly) collocated. The primary coolant system of the test FHR has a cover gas system to remove gaseous and volatile fission products from coolant. In each refueling cycle, the reactor is designed to be operated for 250 full power days (FPDs).

This work was supported by the “Strategic Priority Research Program” of the Chinese Academy of Sciences (No. XDA02050100) and the Scientific Research Foundation for the Returned Overseas Chinese Scholars, State Education Ministry (No. Y519011032).

✉ Kun Chen
chenkun@sinap.ac.cn

¹ Shanghai Institute of Applied Physics, Chinese Academy of Sciences, Shanghai 201800, China

² University of Chinese Academy of Sciences, Beijing 100049, China

Table 1 General parameters of the test FHR developed at SINAP

Item	Specification
Power	10 MW
Coolant	2LiF–BeF ₂
Loading of coolant	2.6 t
Abundance of ⁷ Li in the coolant	99.99%
Moderator and reflector	Graphite
Maximum loading of pebbles	14,650
Fuel kernel temperature	600–700 °C

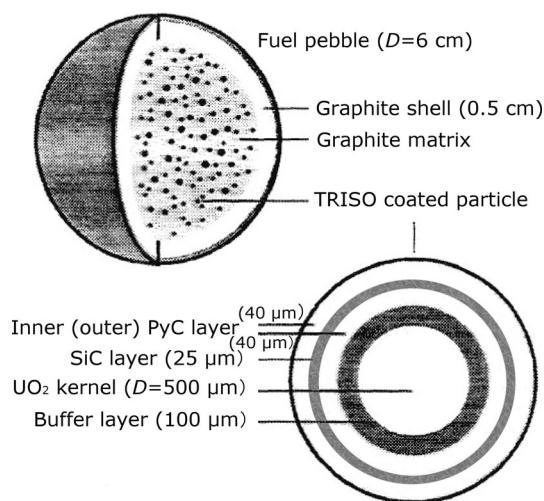


Fig. 1 TRISO-coated particle (bottom) and fuel pebble (top) [5]

Since the design of the test FHR is different from traditional light water reactors or high-temperature reactors, the migration behaviour of radionuclides in the reactor system needs to be investigated to understand the insight of the release mechanisms of radionuclides to the reactor subsystems and to the environment.

2 Origins of radionuclides

Radionuclides in test FHR system are mainly from fission reactions and neutron activations of coolant and structural materials. Fission products such as iodine, noble gases, and some metallic fission products could come out of fuel pebbles and go into the primary coolant through diffusion and leaking processes. The activation of coolant itself and impurities could also produce radionuclides such as ³H, ¹⁴C, ¹⁶N, ¹⁹O, ²⁰F in the coolant system. In addition, activation products of corroded-off Hastelloy-N also exist in the primary coolant system (not being analysed in this work, see Ref. [6] for details).

2.1 Fission products

The SiC layer of the TRISO particle provides retention to fission products both in operation and in accident. However, fission products could still penetrate the coating layer by diffusion or release caused by coating failure. Besides, uranium contamination outside the coating during manufacturing is another dominant source of radionuclides release.

The diffusion of radionuclides can be modelled with physical laws [7], namely the conservation of mass and the Fick’s law .

The conservation of mass can be expressed with the following formula

$$\iiint_V \left(p - \lambda c - \frac{\partial c}{\partial t} \right) dV = \oint_S \vec{j} \cdot d\vec{S}, \tag{1}$$

where V is volume, S is surface area, p is volume specific generation rate, λ is decay constant, c is nuclide concentration, and j is transport flux through outer surfaces.

The diffusion flux and time-dependent change of concentration can be described with the Fick’s law [8] in spherical coordinates as shown below

$$\frac{\partial c}{\partial t} = D \left(\frac{\partial^2 c}{\partial r^2} + \frac{1}{r} \frac{\partial c}{\partial r} \right) - \lambda c + Q, \tag{2}$$

where c is nuclide concentration, D is diffusion coefficient, r is position or radius, λ is decay constant, and Q is fission production rate.

At the surface of the fuel pebble, the boundary condition can be described as [7]

$$-D \frac{\partial c}{\partial r} \Big|_{r=r_s} = \beta (c_{bl} - c_{cl}), \tag{3}$$

where r_s is radius of the pebble, β is mass transfer coefficient from the surface to the coolant, c_{bl} is concentration in the coolant right above the surface of the pebble, an c_{cl} is the mean concentration in the coolant.

The diffusion of fission products is a structure dependent process, and effective diffusion coefficients have been applied with the Fick’s law to describe the overall diffusion process [7].

In the Jülich Research Center, Germany, the STACY code [9] was developed to model the diffusion behaviour in coated particles and fuel pebbles and to estimate the release rate and fraction of fission products. The failed fuel particles are treated as bare UO₂ kernel, while uranium contamination is directly in the graphite matrix. Free evaporation assumption ($\beta \rightarrow \infty$) is applied to account for the release rate from fuel surface to the coolant.

2.2 Activation products

The chemical components of coolant salt, ${}^6\text{Li}$, ${}^7\text{Li}$, and ${}^{19}\text{F}$ could be activated by neutrons through reactions including ${}^6\text{Li}(n, \alpha){}^3\text{H}$, ${}^7\text{Li}(n, n\alpha){}^3\text{H}$, ${}^{19}\text{F}(n, \gamma){}^{20}\text{F}$, ${}^{19}\text{F}(n, \alpha){}^{16}\text{N}$, and ${}^{19}\text{F}(n, p){}^{19}\text{O}$. Activation products of salt include ${}^3\text{H}$ and short-lived nuclides, such as ${}^{16}\text{N}$, ${}^{19}\text{O}$, and ${}^{20}\text{F}$, which will decay and emit gammas. For example, ${}^{20}\text{F}$ emits gammas of 1.64, 2.2 and 2.45 MeV [10] while ${}^{16}\text{N}$ emits gammas of 6.13 and 4.12 MeV [11]. ${}^{20}\text{F}$ and ${}^{16}\text{N}$ have short half lives of about 10 s while it is about 30 s for ${}^{19}\text{O}$.

During manufacturing of the coolant salt, impurities including carbon, nitrogen, and oxygen could be introduced. The reactions of coolant impurities activation include ${}^{13}\text{C}(n, \gamma){}^{14}\text{C}$, ${}^{14}\text{N}(n, p){}^{14}\text{C}$, and ${}^{13}\text{C}(n, \alpha){}^{14}\text{C}$.

The activation of those impurities could produce a certain amount of ${}^{14}\text{C}$, which would exist mostly in the chemical form of oxides, oxycarbides and so on [12].

3 Accumulation in primary coolant

During operation of the reactor, fission products continually enter the primary coolant. Among those fission products, noble gases, iodine, and some metallic fission products could come out the SiC shell of fuel particles. Using the German code STACY, the release rate of fission products could be calculated according to the reactor operation conditions.

On a conservative basis, an assumption was made that radionuclides reach their maximum activities at the beginning of the refueling cycle and remain unchanged. Thus, radionuclides release from fuels with a constant activity per unit time.

The dynamic accumulation process of radionuclides in the primary coolant includes the release of fuel elements, the leak of primary coolant system, and the removal of purification system. A simplified model has been applied to estimate the maximum amount of radionuclide accumulated in the primary coolant system without considering leak and removal mechanism. Based on the release, rate the activities of radionuclides released into the primary coolant can be calculated with the following equation:

$$A_0(t) = c \int_0^t e^{-\lambda_0(t-\tau)} d\tau = \frac{c}{\lambda_0} (1 - e^{-\lambda_0 t}), \quad (4)$$

where $A_0(t)$ is activity of parent nuclide in the coolant, c is activity of nuclide released to the coolant per unit time, λ_0 is decay constant of nuclide, and t is release duration.

Several nuclides, such as ${}^{85\text{m}}\text{Kr}$, ${}^{133\text{m}}\text{Xe}$, and ${}^{135\text{m}}\text{Xe}$, produce ${}^{85}\text{Kr}$, ${}^{133}\text{Xe}$, and ${}^{135}\text{Xe}$ through decay, and the

daughter nuclides decay, too. The radioactivity of daughter nuclides can be calculated with the following equation:

$$\begin{aligned} A_1(t) &= \int_0^t \lambda_1 f_1 A_0(\tau) e^{-\lambda_1(t-\tau)} d\tau \\ &= \int_0^t \lambda_1 f_1 \frac{c}{\lambda_0} (1 - e^{-\lambda_0 \tau}) e^{-\lambda_1(t-\tau)} d\tau \\ &= \frac{cf_1}{\lambda_0} (1 - e^{-\lambda_1 t}) - \frac{\lambda_1}{\lambda_0} \frac{cf_1}{\lambda_1 - \lambda_0} (e^{-\lambda_0 t} - e^{-\lambda_1 t}), \end{aligned} \quad (5)$$

where $A_1(t)$ is activity of first generation daughter nuclide in the coolant, f_1 is decay fraction of parent nuclide to daughter nuclide, and λ_1 is decay constant of daughter nuclide.

${}^{133}\text{I}$ and ${}^{135}\text{I}$ produce ${}^{133\text{m}}\text{Xe}$ and ${}^{135\text{m}}\text{Xe}$ while ${}^{133\text{m}}\text{Xe}$ and ${}^{135\text{m}}\text{Xe}$ produce ${}^{133}\text{Xe}$ and ${}^{135}\text{Xe}$ by decay. The radioactivity of second-generation daughter nuclides can be calculated with the following equation:

$$\begin{aligned} A_2(t) &= \int_0^t \lambda_2 f_2 A_1(\tau) e^{-\lambda_2(t-\tau)} d\tau \\ &= \int_0^t \lambda_2 f_2 \left(\frac{cf_1}{\lambda_0} (1 - e^{-\lambda_1 \tau}) - \frac{\lambda_1}{\lambda_0} \frac{cf_1}{\lambda_1 - \lambda_0} (e^{-\lambda_0 \tau} - e^{-\lambda_1 \tau}) \right) \\ &\quad e^{-\lambda_2(t-\tau)} d\tau \\ &= cf_1 f_2 \left(\frac{1 - e^{-\lambda_2 t}}{\lambda_0} + \frac{\lambda_2}{\lambda_1 - \lambda_0} \frac{e^{-\lambda_1 t} - e^{-\lambda_2 t}}{\lambda_2 - \lambda_1} \right. \\ &\quad \left. - \frac{\lambda_2}{\lambda_0} \frac{\lambda_1}{\lambda_1 - \lambda_0} \frac{e^{-\lambda_0 t} - e^{-\lambda_1 t}}{\lambda_2 - \lambda_0} \right), \end{aligned} \quad (6)$$

where $A_2(t)$ is activity of the second-generation daughter nuclide in the coolant, f_2 is decay fraction of first generation daughter nuclide to second-generation daughter nuclide, and λ_2 is decay constant of second-generation daughter nuclide.

4 Results and discussions

4.1 Results

After 250 FPDs, calculated inventory of key radionuclides, that could be potentially released from fuel pebbles, in the fuels are listed in Table 2. The calculations were performed using TRITON and ORIGEN-S modules of SCALE 6.1 package [13].

TRITON produced problem dependent burn-up library for the test FHR, and ORIGEN-S has been used to calculate inventory and for activation analysis.

STACY codes have been used to calculate the release rate (Table 3) according to the design parameters of the test FHR. The calculated release rate is a sum of effects including diffusion, coating failure, and uranium

Table 2 Inventory of key radionuclides at the end of refueling cycle, 250 FPDs

Nuclides	Activity (Bq)	Nuclides	Activity (Bq)
^3H	1.29×10^{12}	^{131}I	9.24×10^{15}
$^{83\text{m}}\text{Kr}$	1.62×10^{15}	^{132}I	1.39×10^{16}
^{85}Kr	4.12×10^{13}	^{133}I	2.11×10^{16}
$^{85\text{m}}\text{Kr}$	3.77×10^{15}	^{134}I	2.44×10^{16}
^{87}Kr	7.68×10^{15}	^{135}I	1.97×10^{16}
^{88}Kr	1.03×10^{16}	$^{131\text{m}}\text{Xe}$	1.01×10^{14}
^{89}Sr	1.38×10^{16}	^{133}Xe	2.02×10^{16}
^{90}Sr	3.00×10^{14}	$^{133\text{m}}\text{Xe}$	6.16×10^{14}
^{134}Cs	7.20×10^{13}	^{135}Xe	7.68×10^{15}
^{137}Cs	3.16×10^{14}	$^{135\text{m}}\text{Xe}$	3.98×10^{15}
^{88}Rb	1.04×10^{16}		

Table 3 Calculated release rate

Nuclide	Half-live	Release rate (s^{-1})
$^{83\text{m}}\text{Kr}$	1.83 h	5.28×10^{-10}
^{85}Kr	10.76 a	7.45×10^{-13}
$^{85\text{m}}\text{Kr}$	4.48 h	2.17×10^{-10}
^{87}Kr	76.3 min	7.58×10^{-10}
^{88}Kr	2.80 h	1.30×10^{-11}
$^{131\text{m}}\text{Xe}$	12.0 d	4.66×10^{-12}
^{133}Xe	5.29 d	9.26×10^{-12}
$^{133\text{m}}\text{Xe}$	2.2 d	2.02×10^{-11}
^{135}Xe	9.17 h	1.07×10^{-10}
$^{135\text{m}}\text{Xe}$	15.3 min	3.75×10^{-9}
^{131}I	8.04 d	6.49×10^{-12}
^{132}I	2.38 h	4.07×10^{-10}
^{133}I	20.8 h	4.85×10^{-11}
^{134}I	52.0 min	1.11×10^{-19}
^{135}I	6.59 h	1.49×10^{-10}
^{134}Cs	2.06 a	2.10×10^{-14}
^{137}Cs	30.1 a	2.03×10^{-14}
^{88}Rb	17.8 min	5.59×10^{-13}
^{89}Sr	50.5 d	1.37×10^{-17}
^{90}Sr	28.5 a	1.36×10^{-17}
$^{110\text{m}}\text{Ag}$	250.4 d	1.36×10^{-13}

contamination. Effective diffusion coefficients of cesium, strontium, silver, and noble gases are taken from Refs. [7, 14]. For those nuclides lacking diffusion coefficients, the data of chemically similar nuclides have been applied. For example, the diffusion coefficients of cesium were used for rubidium. Since the pebble fuel produced in China, which was originally developed for high-temperature gas-cooled demonstration reactor, is planned to be used in the test FHR. For the amount of uranium contamination (5.0×10^{-6}) and the particle failure rate

(6.0×10^{-5}) refer to the data of HTR-10 and HTR-PM fuel elements [15, 16].

Based on the results shown in Tables 2 and 3, the activity of radionuclides released from fuel pebbles to the coolant can be calculated with Eqs. (4)–(6). After 250 FPDs, the amount of fission products are listed in Table 4.

Based on the experiences of MSRE, 100% of noble gases, 10% of iodine, and 10% of solid fission products (such as metallic fission products) would be released from the salt [17], and the rest of the nuclides remain in the primary coolant. Noble gases are in the form of elementary gases. Iodine after released from the salt is in the form of iodine ion or I_2 , and metallic fission products are in the form of the fluorides [18].

Activation products of coolant and impurities are shown in Table 5. In the calculation, the contents of nitrogen, carbon, and oxygen impurities were selected as 100 ppm wt according to reactor design requirements.

4.2 Discussions

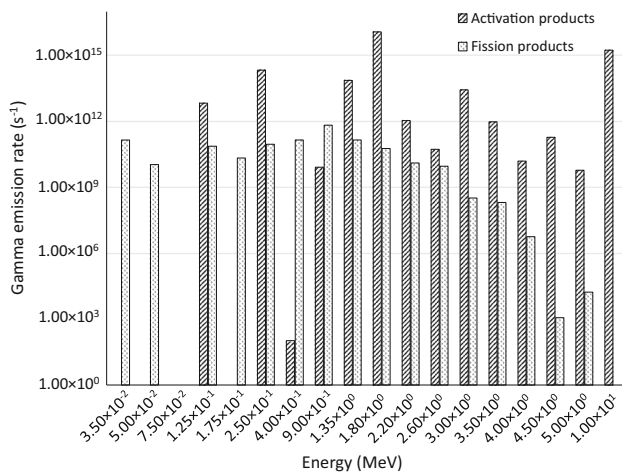
During operation of the reactor, the activity of activation products in the primary coolant system is several orders of magnitude higher than that of fission products (Tables 4, 5). As shown in Fig. 2, gammas are mainly from activation products, and those short-lived activation products (^{16}N ,

Table 4 Fission products accumulated in primary coolant system (250 FPDs)

Category	Nuclide	Activity (Bq)	
Noble Gases	$^{83\text{m}}\text{Kr}$	8.13×10^9	
	^{85}Kr	8.24×10^8	
	$^{85\text{m}}\text{Kr}$	1.91×10^{10}	
	^{87}Kr	3.86×10^{10}	
	^{88}Kr	1.95×10^9	
	$^{131\text{m}}\text{Xe}$	1.37×10^9	
	^{133}Xe	2.37×10^{11}	
	$^{133\text{m}}\text{Xe}$	3.61×10^9	
	^{135}Xe	1.60×10^{11}	
	$^{135\text{m}}\text{Xe}$	3.63×10^{10}	
	Iodine	^{131}I	6.01×10^{10}
		^{132}I	6.94×10^{10}
		^{133}I	1.11×10^{11}
^{134}I		1.21×10^{11}	
^{135}I		1.01×10^{11}	
Metallic fission products	^{134}Cs	2.72×10^7	
	^{137}Cs	1.32×10^8	
	^{88}Rb	8.95×10^6	
	^{89}Sr	1.16×10^6	
	^{90}Sr	8.78×10^4	
	$^{110\text{m}}\text{Ag}$	7.59×10^5	

Table 5 Activities of activation products in primary coolant system (250 FPDs)

Nuclides	Activity (Bq)
^3H	1.73×10^{15}
^{14}C	2.87×10^{10}
^{16}N	2.95×10^{15}
^{19}O	2.44×10^{14}
^{20}F	1.15×10^{16}

**Fig. 2** Gamma flux spectra of radionuclides in primary coolant at the end of the refueling cycle (250 FPDs)

^{20}F) emitting high energy gammas should be considered in shielding design work of the test FHR. After shutdown, short-lived nuclides decay quickly and disappear shortly, while the activity of long-lived nuclides decreases slowly.

Among those radionuclides accumulated in the primary coolant system, the release of ^3H and ^{14}C need to be paid more attention during normal operation as they can be released to the environment and result in exposure to surrounding residents through ground-shine, immersion, and food chain. ^3H production rate of the test FHR is about 0.69 TBq/MWd while it is about 0.05 TBq/MWd for CANDU 6 reactor [19]. ^{14}C production rate of the test FHR is about 1.15×10^7 Bq/MWd. Normalized to 3000 MW, both ^3H and ^{14}C produced in the test FHR exceed the release limits in “Regulations for environmental radiation protection of nuclear power plant” (GB 6249-2011). Therefore, treatment of ^3H and ^{14}C should be considered.

^3H originates mainly from the activation of ^6Li and ^7Li [20]. According to the results in Table 6, which were calculated according to the neutron spectrum of the test FHR obtained with Monte Carlo simulation, ^3H production cross section of ^6Li is about 2.0×10^5 times higher than that of ^7Li . Although the amount of ^6Li in the coolant is much lower (Table 1), it is still the dominant ^3H production source. ^{14}C has several sources including the activation of

Table 6 Effective cross section of neutron activation reactions in the test FHR coolant

Reaction	Cross section (barns)
$^6\text{Li}(n, \alpha)^3\text{H}$	1.82×10^2
$^7\text{Li}(n, n\alpha)^3\text{H}$	9.10×10^{-4}
$^{13}\text{C}(n, \gamma)^{14}\text{C}$	3.13×10^{-4}
$^{14}\text{N}(n, p)^{14}\text{C}$	3.55×10^{-1}
$^{17}\text{O}(n, \alpha)^{14}\text{C}$	5.39×10^{-2}

^{13}C , ^{14}N , and ^{17}O . Since the cross section of $^{14}\text{N}(n, p)^{14}\text{C}$ is the highest, it is the dominant source of ^{14}C .

5 Conclusion

The amount of radionuclides accumulated in the primary coolant system of a test FHR has been analysed in this work. The release of fission products from fuel elements to the coolant system was considered, as well as the neutron activation of the coolant itself and impurities. A simplified model, which did not take leak and removal mechanism into account, was used to account for the decay and accumulation of released radionuclides. According to the analysis, several conclusions could be made as follows:

1. During operation, short-lived activation products of the coolant are a much stronger radiation source than fission products.
2. ^3H and ^{14}C originate from the activation of coolant and impurities, respectively. Because of their high specific production rates, ^3H and ^{14}C should be treated and monitored before being released to the environment in order to comply with the regulation of authorities.
3. ^6Li in the coolant of the test FHR is a dominant ^3H production source. Efforts should be made to reduce the content of ^6Li to avoid high production rate of ^3H .
4. ^{14}N could be introduced into the coolant during manufacturing; it should be reduced as it is the dominant ^{14}C production source.

This work is to give a first glimpse of the radionuclides migration mechanism in a pebble-bed FHR system. Since simplified models and assumptions were applied, further investigation has to be made theoretically and experimentally to gain additional insights.

References

1. C.W. Forsberg, P.F. Peterson, P.S. Pickard, Molten-salt-cooled advanced high-temperature reactor for production of hydrogen

- and electricity. Nucl. Technol. **144**, 289–302 (2003). doi:[10.13182/NT03-1](https://doi.org/10.13182/NT03-1)
2. M.J. Wang, R.J. Sheu, J.J. Peir et al., Criticality calculations of the HTR-10 pebble-bed reactor with SCALE6/CSAS6 and MCNP5. Ann. Nucl. Energy **64**, 1–7 (2014). doi:[10.1016/j.anucene.2013.09.031](https://doi.org/10.1016/j.anucene.2013.09.031)
 3. M.D. Mei, S.W. Shao, Z.Z. He et al., Research on initial event analysis for solid thorium molten salt reactor probabilistic safety assessment. Nucl. Tech. **37**, 090601 (2014). doi:[10.11889/j.0253-3219.2014.hjs.37.090601](https://doi.org/10.11889/j.0253-3219.2014.hjs.37.090601)
 4. K. Verfondern, H. Nabielek, J.M. Kendall, Coated particle fuel for high temperature gas cooled reactors. Nucl. Eng. Technol. **39**, 603–616 (2007). doi:[10.5516/NET.2007.39.5.603](https://doi.org/10.5516/NET.2007.39.5.603)
 5. C. Yang, C. Fang, J. Zhang et al., Study on cumulative fractional release of radionuclides in HTGR fuel particles. Acta. Phys. Sin. **63**, 032802 (2014). doi:[10.7498/aps.63.032802](https://doi.org/10.7498/aps.63.032802)
 6. C. Peng, X.W. Zhu, G.Q. Zhang et al., Numerical analysis of the activity of irradiated alloy-N in TMSR-SF1. Nucl. Sci. Tech. **27**, 44 (2015)
 7. K. Verfondern, H. Nabielek, in *FRESCO-II Verification and Validation* (Research Center Juelich, Juelich, Germany, 2012)
 8. J. Crank, *The Mathematics of Diffusion*, 2nd edn. (Oxford University Press, New York, 1975)
 9. A. Xhonneux, H.J. Allelein, Development of an integrated fission product release and transport code for spatially resolved full-core calculations of V/HTRs. Nucl. Eng. Des. **271**, 361–369 (2014). doi:[10.1016/j.nucengdes.2013.11.063](https://doi.org/10.1016/j.nucengdes.2013.11.063)
 10. J.V. Jelley, The radioactivity of fluorine 20. Proc. Phys. Soc. A **63**, 538–539 (1950)
 11. D.E. Alburgeck, Beta decay of N-16. Phys. Rev. **111**, 1586–1590 (1958). doi:[10.1103/PhysRev.111.1586](https://doi.org/10.1103/PhysRev.111.1586)
 12. X.W. Zhu, S. Wang, C. Peng et al., Production and release of ^{14}C in TMSR-SF1. Nucl. Tech. **38**, 030603 (2015). doi:[10.11889/j.0253-3219.2015.hjs.38.030603](https://doi.org/10.11889/j.0253-3219.2015.hjs.38.030603) (in Chinese)
 13. ORNL, in *Scale: A Comprehensive Modelling and Simulation Suite for Nuclear Safety Analysis and Design* (Oak Ridge National Laboratory, Oak Ridge, Tennessee, 2011)
 14. IAEA, in *Fuel Performance and Fission Product Behaviour in Gas Cooled Reactors* (International Atomic Energy Agency, Vienna, 1997)
 15. J.Z. Cao, S.R. Xi, Study on retaining performance of fuel element and coated particles to fission products in HTGR. Nucl. Power Eng. **20**, 440–443 (1999)
 16. X.W. Zhou, Z.M. Lu, J. Zhang et al., Research and manufacture of spherical fuel element for HTR-PM demonstration project. Atom. Energy Sci. Tech. **48**, 1228–1233 (2014). doi:[10.7538/yzk.2014.48.07.1228](https://doi.org/10.7538/yzk.2014.48.07.1228)
 17. S.E. Beall, P.N. Haubenreich, R.B. Lindauer et al., in *MSRE Design and Operations Report Part V—Reactor Safety Analysis Report*, vol. 732 (Oak Ridge National Laboratory, Oak Ridge, Tennessee, 1964)
 18. E.L. Compere, S.S. Kirslis, E.G. Bohlmann et al., in *Fission Product Behaviour in the Molten Salt Reactor Experiment* (Oak Ridge National Laboratory, Oak Ridge, Tennessee, 1975)
 19. J. Zhang, H.W. Li, Analysis of effluence tritium release from Qinshan phase III heavy water reactor. Radiat. Prot. **29**, 80–85 (2009)
 20. C. Peng, X.W. Zhu, G.Q. Zhang et al., Comparison among SCALE packages applied to the analysis of tritium in an FHR. Nucl. Tech., **38**:080601 (2015). doi:[10.11889/j.0253-3219.2015.hjs.38.080601](https://doi.org/10.11889/j.0253-3219.2015.hjs.38.080601) (in Chinese)